Tp.

STUDY OF THE RELATIONSHIP OF PROPERTIES OF COMPOSITE MATERIALS TO PROPERTIES OF THE.R CONSTITUENTS

N64-26577

Code-1 Cat-34

NASA CR-58182

Quarterly Progress Report No. 3
July 24, 1964
Contract NASw-817
GE Requisition 214-W42

Prepared for:
National Aeronautics and Space Administration
Washington, D.C.

Prepared by:
Norris F. Dow, Zvi Hashin* and B. Walter Rosen
Space Sciences Laboratory
General Electric Company
P.O. Box 8555
Philadelphia 1, Pennsylvania

*University of Pennsylvania
Philadelphia, Pennsylvania

Table of Contents

SUMMARY

26577

Third quarter progress in the study of the influence of constituent properties upon composite performance is described. Parametric studies of the influence of geometry and properties of fiber and matrix upon the structural efficiency of cylindrical sandwich shells in axial compression are presented. Analytical and experimental studies of elastic constants and tensile strength of modified matrix materials are also included.

Author

INTRODUCTION

The previous contract studies of composites for compressive applications have indicated the potential of advanced composites in the form of sandwich wall cylindrical shells. The present report describes the status of more definitive studies to determine the influence of constituent geometry and properties upon the structural efficiency of composites for conditions typical of boost vehicle tanks.

These studies have indicated that in certain cases variation of matrix properties can result in reduction of structural weight. Progress on the experimental and analytical studies of the variation of matrix properties are also described herein. These include further consideration of the elastic constants, treatment of transverse composite strength by the methods of limit analysis and experimental study of stiffness and strength changes produced by chemical modifications and use of small particle fillers in epoxy matrix materials.

ELASTIC MODULI OF FIBROUS COMPOSITES OF ARBITRARY TRANSVERSE GEOMETRY

The previous contract studies of the elastic moduli of transversely isotropic fibrous composites (Ref. 1 and 2) resulted in expressions and bounds for these moduli for certain types of geometry. The most important results were obtained for a special geometry which is described by a fiber-reinforced material which consists entirely of parallel composite cylinders. Each composite cylinder consists of a fiber core, which may be hollow, and of a concentric binder cylindrical shell. The cross section sizes diminish from finite to infinitesimal sizes and thus the remaining binder volume, not included in cylinders, may be made arbitrarily small. These results were also applied, subject to a geometric approximation, to the case of randomly distributed equal diameter fibers.

By a variational bounding method based on the classical principles of minimum potential energy and minimum complementary energy, expressions for four effective elastic moduli were obtained. These moduli are K_{23}^* -the plane strain bulk modulus referred to the transverse 23 plane (normal to the fibers), G_1^* -the shear modulus governing shear in a plane normal to the transverse plane (parallel to the fibers) E_1^* -the Young's modulus for uniaxial stress in fiber direction and ν_1^* -the Poisson's ratio for the same case. The fifth elastic modulus G_{23}^* -shear modulus in the transverse plane could only be bounded from below and above.

The above mentioned results are valuable as approximate expressions and they have been used herein in extensive parametric structural efficiency studies. There are, however, certain remaining unanswered questions associated with the elastic constants of fibrous composites. Principal among these is the effect of non-uniform fiber spacing. One method of assessing the possible magnitude of effects associated with this uncertain transverse geometry is to determine bounds on the elastic constants for arbitrary transverse geometry. This will also provide information for consideration of non-circular fibers.

An alternate approach is to apply statistical techniques to the problem of specifying transverse geometry. This may be done in terms of joint probability functions. To give an example, let it be assumed that the fibers have full cross sections (no voids). Consider two arbitrary points $\underline{x}^{(1)}$ and $\underline{x}^{(2)}$ in a transverse plane. The distance between the points is given by

$$\underline{r} = \underline{x}^{(2)} - \underline{x}^{(1)} \tag{1}$$

One may now define four two point probabilities. For example, g^{11} is the probability that both points are in phase one (say binder) g^{12} is the probability that the first point is in phase one (binder) and the second in phase two (fibers). Analogously one has the joint probabilities g^{21} and g^{22}. Let these probabilities be denoted shortly by g^{mn}. The assumption of statistical homogeneity of the material implies

$$g^{mn} = g^{mn}(\underline{r}) \tag{2}$$

that is to say the actual position of the two points in the material is of no consequence. The further assumption of statistical transverse isotropy implies that for $\underline{r}$ in the transverse plane:

$$g^{mn} = g^{mn}(r) \tag{3}$$

where r is the magnitude of $\underline{r}$. Eq. (3) means that the actual direction of $\underline{r}$ in the transverse plane is of no consequence. For $\underline{r}$ not in the transverse plane, the joint probability functions remain functions of $\underline{r}$.

In the same way one may define three point, four point ... and N point joint probabilities. As more and more joint probabilities are known the statistical geometry becomes more and more specified. In general the joint probabilities must be determined by experiment.

It is interesting to note the meaning of one point probabilities. These are the probabilities that a point thrown at random into the material is either in one or the other phase. It is easy to realize that the one point probabilities are just the volume fractions of the phases.

The general definition of the effective elastic moduli C^{*}_{ijkl} is

$$\bar{\sigma}_{ij} = C_{ijkl} \; \bar{\varepsilon}_{kl} \tag{4}$$

where the range of subscripts is 1, 2, 3, a repeated subscript denotes summation and overbars denote average values over large volume elements. Eq. (4) is meaningful only for boundary displacements or loadings which produce uniform states of stress and strain in homogeneous media, (1, 2). In the present case of statistical transverse isotropy there are five independent effective elastic moduli, for example the one listed above.

In general the effective elastic moduli are functions of the phase moduli and the phase geometry. For random geometry they are thus functions of all the N point joint probability functions of all orders. It is at present not known how to establish this functional relationship in general. The present analysis is concerned with a simpler yet very important question: Given only phase moduli and phase volume fractions, (i.e. one point averages), to what extent are the effective elastic moduli defined by such information? Such information will henceforth be referred to as simplest information. The present method of investigation is again a variational bounding method which is, however, based on new variational principles in the classical theory of elasticity (Ref. 3). The bounding method is also based on statistical analysis.

The details of the analysis which is quite lengthy will be given elsewhere. Here only the final results will be stated. With the notation employed in Ref. 1 and 2 and for a material consisting of full elastic fibers and an elastic binder the bounds are:

For K^*_{23}

$$K^{*(-)}_{23} = K_b + \frac{v_f}{\dfrac{1}{K_f - K_b} + \dfrac{v_b}{K_b + G_b}} \tag{5}$$

$$K^{*(+)}_{23} = K_f + \frac{v_b}{\dfrac{1}{K_b - K_f} + \dfrac{v_f}{K_f + G_f}}$$

For G^*_{23}

$$G^{*(-)}_{23} = G_b + \frac{v_f}{\dfrac{1}{G_f - G_b} + \dfrac{(K_b + 2G_b)v_b}{2G_b(K_b + G_b)}}$$

$$G^{*(+)}_{23} = G_f + \frac{v_b}{\dfrac{1}{G_b - G_f} + \dfrac{(K_f + 2G_f)v_f}{2G_f(K_f + G_f)}} \tag{6}$$

For G^*_1

$$G^{*(-)}_1 = G_b + \frac{v_f}{\dfrac{1}{G_f - G_b} + \dfrac{v_b}{2G_b}}$$

$$G^{*(+)}_1 = G_f + \frac{v_b}{\dfrac{1}{G_b - G_f} + \dfrac{v_f}{2G_f}} \tag{7}$$

R. Hill has obtained bounds for E^*_1 and ν^*_1 of transversely isotropic fiber reinforced materials in terms of volume fractions and phase moduli only by different methods, (private communication, to be published). His bounds show that from a practical point of view the law of mixtures is in general a good approximation. Similar conclusions have been reached in Refs. 1 and 2. Thus good approximations for E^*_1 and ν^*_1 are:

$$E_1^* \approx E_b v_b + E_f v_f \tag{8}$$

$$\nu_1^* \approx \nu_b v_b + \nu_f v_f \tag{9}$$

It has been shown that the bounds (5), (7) and also Hill's bounds are best possible in terms of phase moduli and phase volume fractions. By this is meant: If the only information available is the simplest information then these bounds give the best information one may possibly obtain about the effective elastic moduli. Obviously, in order to improve the bounds one has to use additional information such as two point and higher order joint probabilities. It is as yet not known how to use such information. It is not yet known whether the bounds (6) are also best possible in terms of the simplest information, however, the method of derivation suggests that it is possible that they are.

The nature of the bounds described above is of considerable practical significance. A designer of a fiber reinforced material certainly knows the elastic moduli of the constituents from experiments and also has control over the volume fractions. He has, however, no control over the higher order statistical details of the geometry. Therefore, the usual method of manufacture of such materials must invariably lead to scatter in the effective elastic moduli. The worst possible amount of scatter is defined by the bounds given above. Unfortunately, the distance between the bounds is quite large. This is to be expected as the arbitrary phase geometry includes the extremes of each material being either matrix or inclusion. The arbitrary phase

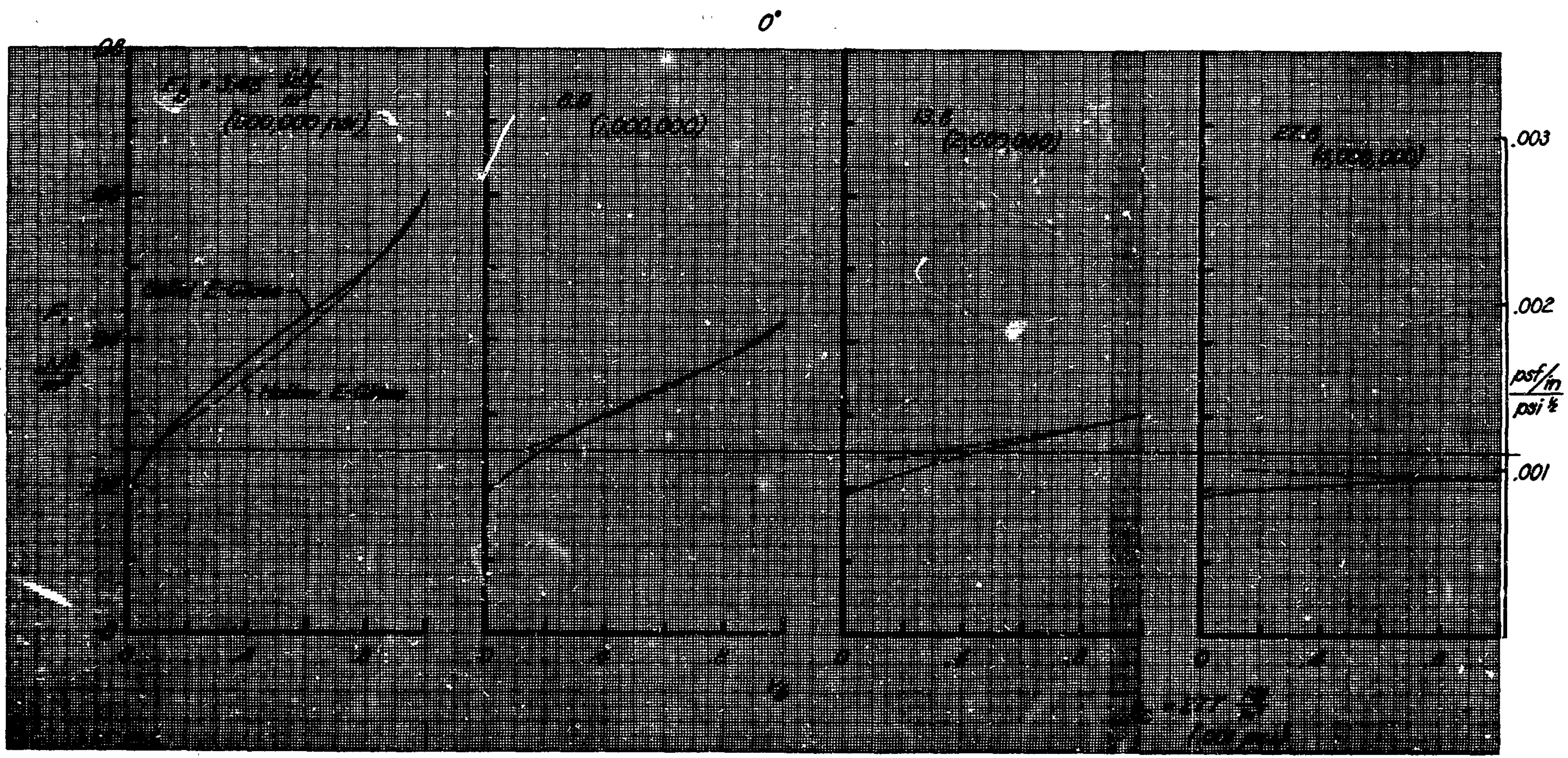

Figure 7. Comparison of the Elastic Buckling Efficiencies of Solid and Hollow-Fiber Reinforced Composites for Sandwich Shells in Compression: Case I. Filaments in the Axial (loaded) Direction Only.

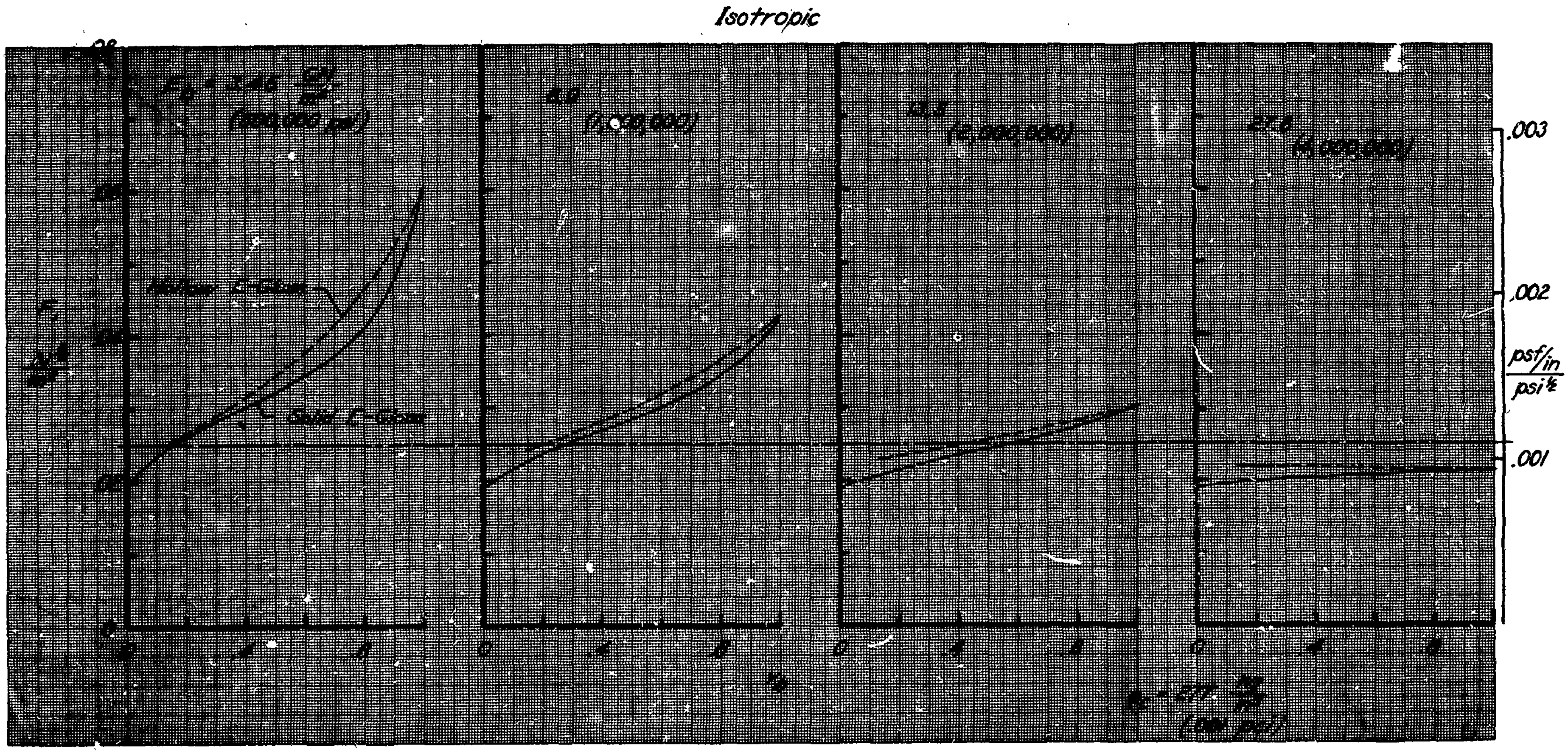

Figure 8. Comparison of the Elastic Buckling Efficiencies of Solid and Hollow-Fiber Reinforced Composites for Sandwich Shells in Compression: Case II. Laminates with Filaments at $\pm$ 30° and 180° to the Axial (Loaded) Direction.

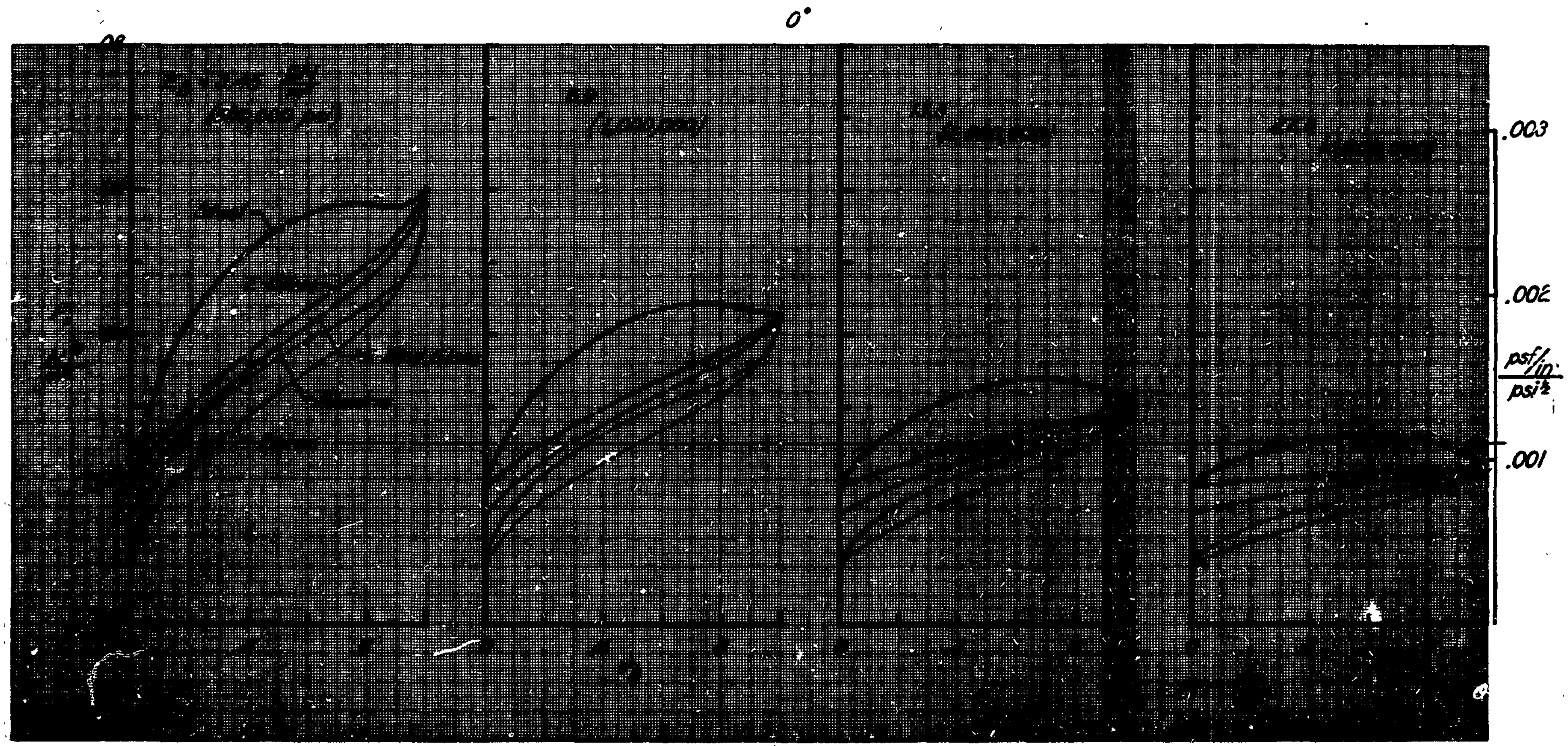

Figure 5. Relative Efficiencies for Elastic Buckling of Composites for Sandwich Construction of Cylindrical Shells in Compression: Case I. Filaments in the Axial (Loaded) Direction only.

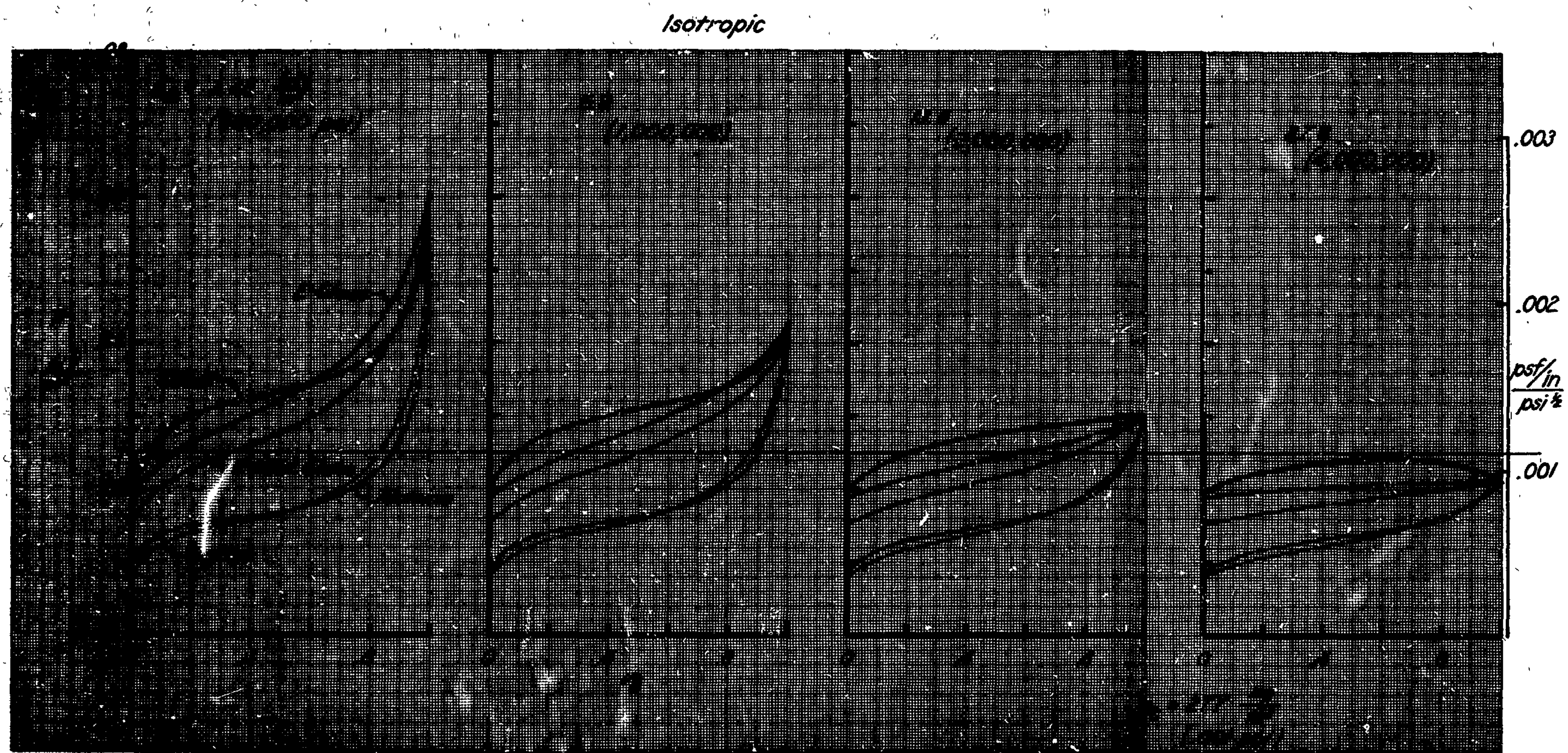

Figure 6. Relative Efficiencies for Elastic Buckling of Composites for Sandwich Construction of Cylindrical Shells in Compression: Case II. Laminates with Filaments at ± 30° and 180° to the Axial (Loaded) Direction.

geometry bounds are compared to the previous random array bounds for the transverse shear modulus in Fig. 1. It is seen that, for all but small ratios of constituent moduli, the arbitrary geometry bounds are extremely far apart. An interesting and unexpected result is that the lower bound for arbitrary transverse geometry is higher than the lower bound obtained in Ref. 1 and 2 for circular fibers in a random array. This arbitrary geometry lower bound has therefore been substituted into the existing elastic constants computer program, resulting in a reduction in the distance between the previous bounds on transverse Young's modulus.

EXPERIMENTAL STRESS-STRAIN RELATIONS

A preliminary study of the range of matrix properties available by perturbing the composition of a standard epoxy was undertaken. These results are a first step in the experimental study of the influence of matrix properties upon composite properties.

Preliminary investigations were made on the following formulations:

Series	Kopoxite 159	MNA	EM207	BDMA
17	100	125	--	1
1&2	100	125	25	1
14	100	125	50	1
19	100	125	75	1

Since Kopoxite 159 (a relatively pure resorcinol diglycidyl ether) tended to crystallize on standing at room temperature, the formulations were usually made by first melting the Kopoxite 159, then stirring in the other components until a homogeneous mixture was schieved. After vacuum de-aeration, the formulation was cast into a 1/4" mold and cured at elevated temperatures. After curing, the 1/4" sheet of resin was cut into tensile specimens and tested for physical characteristics on the Instron machine, using a cross-head speed of .05 in./min. Fig. 2 compares the properties of these first four formulations. It is of interest to note the large increase in elongation achieved by increasing the EM207 (a glycol adipate polyester) content from 50 to 75 parts. There is little question but that a critical concentration region lies between these two concentrations.

Further investigations were undertaken using Kopoxite 159 and a number of anhydride curing agents and polymeric modifiers. The following table lists these formulations:

Series	Kopoxite 159	Methyl Nadic Anhydride	BDMA	MA	Harcure E
20	100		1	65	
21	100	80	1		102

These materials were prepared in order to determine the effect of various molecular constituents on the physical properties of epoxy castings. Formulation 20, darkened considerably upon curing, and was quite brittle. Formulation 21 was soft and flexible.

The tensile data obtained on these two materials are listed in the table below:

Series	Ultimate Tensile Strength KSI	Young's Modulus PSI	Elongation %
20	13.6 - 13.8	$0.503\text{-}0.557 \times 10^6$	5.3-8.9
21	0.9	$.095 \times 10^6$	25%

These data illustrate the extreme flexibility that can be achieved using an adipate glycol flexibilizer of the Harcure "E" type (Note, Harcure E is a polyester of adipic acid, 1, 4 - butanediol, and propylene glycol, containing excess acid groups). Also a new resin system, ERRA0300, was investigated to obtain a high strength high modulus formulation. The initial results were disappointing as shown below and this aspect of the variation of matrix properties will be pursued.

Series 25

ERRA	94.2 pbw
Maleic anhydride	83.5 pbw
Trimethyl propane	9.0 pbw

U.T.S.	6.15-7.50 ksi
Failure strain	2.4-5.4%

Effect of Fillers

Aluminum flake, aluminum powder, and aluminum needles were investigated. Leafing grade aluminum flake was incorporated into Series 1 and 2 to the extent of 30% of volume, and approximately 50% by weight. The result was a very thick, pasty mass that was impossible to de-aerate using vacuum techniques, even when accompanied by vibration. Further attempts to deaerate other specimens of this same composition were made using centrifugation. These attempts also resulted in failure, since cured specimens that had been subjected to centrifuging at 20,000 RPM exhibited large, lens shaped and irregular voids normal to the applied centrifugal force. These difficulties were attributed to the tendency of the flake aluminum to overlap and bridge, in addition to the thixotropic effect of the finely divided particles.

Almeg PF Aluminum needles have undergone a preliminary investigation in which specimens of the needles (.27" length by .028" to .032" diameter) were encapsulated in Series 19 resin. Encapsulation was accomplished by first spreading a layer of needles 1/4" deep in a flat pan, pouring resin on top, then deaerating under vacuum. After curing, the specimens were cross sectioned and a number of voids were observed dispersed throughout the composite mass. In an attempt to eliminate the voids, other composites were made in which deaerated resin was mixed with aluminum needles, the composite spread out in a layer 1/2" thick, further de-aerated, then cured. This technique was also unsuccessful in producing void-free pieces. The voids in all cases appeared to be distributed randomly throughout the piece, but were concentrated in some areas around the points of the aluminum needles, which serve as nucleation centers for gases.

Aluminum powder was used as a filler in combination with Series 19 resin. The powder was Fisher Laboratory's "Aluminum Metal-Finest Powder" (catalog number A-559). The aluminum powder was used as received in one formulation, washed with ligroine and acetone in another, and coated with a mold release agent in a third. An unfilled casting of Series 19 resin was also prepared and used as a control during subsequent mechanical testing of the filled castings.

In the preparation of the filled specimens, it was soon learned that a filler concentration of 66% by weight could be easily achieved without producing a material that was thixotropic or too difficult to handle, so this concentration was adopted as standard throughout this phase of the investigation.

The following table lists the formulation, filler, and filler treatments investigated:

Powder Aluminum - Resin Composites

Series	Type of Casting	Treatment of Aluminum
19	Unfilled Resin Control	None
18	Aluminum Filled Casting	As received
22	" " "	Washed in acetone/ligroine
23	" " "	Coated with mold release

These castings were prepared, de-aerated, and cured in as uniform a fashion as possible, so as to minimize differences between them other than those inserted by experimental design. After curing, the castings were machined into tensile specimens and tested, with results as shown in Table I.

It is apparent from an examination of these data that the addition of the powdered aluminum filler, no matter what the treatment, to the resin resulted in a lowered ultimate tensile strength in the composite, along with a decrease in the elongation to failure, and an increase in modulus. Washing the filler with acetone and ligroine improved the properties of the composite slightly, and coating the filler with a mold release agent caused a further deterioration of properties.

The second phase of this study was concentrated upon resorcinal diglycidal ether based formulations essentially the same as series 1 & 2 (PJ 122) using filled and unfilled resins. Table I outlines the formulations and fillers used and gives mechanical property results obtained on test specimens made from castings.

An examination of the data in Table I shows that neither the A1100 or 26020 surface active agents improved the adhesion of the epoxy resin to the aluminum particles, as evidenced by the decrease in tensile strength of the filled resin when compared to the unfilled resin. The formulation containing 26020 displayed slightly better properties than the formulation containing A1100. Wide variation was displayed in the properties of the composite formulation when decreased aluminum particles were used in conjunction with resin containing no surface active agent.

Some interesting results were obtained when composites made of conversion coated (Detrex/Chromate Etch) aluminum powder filled resins were tested. The composite (Series 30 and 12A-28-2) made using a relatively low modulus (Ca 2.5 - 3.0 x 10^5psi) resin showed an increase in tensile strength when compared to the unfilled resin. On the other hand, the composite (Series 12A-29-5) made using a relatively high modulus (Ca 5 x 10^5psi) resin showed a drastic decrease in tensile strength when compared to the unfilled resin. The results of this latter test, it should be noted, are somewhat in doubt because the presence of small bubbles in the matrix is suspected.

Series 20 resin displayed remarkably uniform properties, but was only a slight improvement in tensile strength over the previously tested Series 1 & 2 materials. Series 25, based upon a totally new resin system, was disappointingly poor.

PLASTIC LIMITING LOADS FOR SOME FIBER REINFORCED OR PARTICLE REINFORCED MATERIALS

The problem of the strength of fiber reinforced materials and composite media in general is one of the most important aspects of the study of mechanical behavior of such media. Ideally speaking the aim is to predict mechanical behavior and strength of the composite on the basis of the known mechanical behavior and the geometry of the constituents. The present investigation is concerned with limited treatment of this problem by use of the theorems of limit analysis of the theory of plasticity, for cases where the load is applied in a direction such that there is no continuous load path through the inclusions.

Theorems of Limit Analysis

The theorems of limit analysis are concerned with the evaluation of the limiting or ultimate load which can be carried by plastic bodies. The limiting load is defined as that load at which the deformation of the body can increase without increase in load. This load may be defined as the failure load of the body.

One way to find the limiting load is to find the stresses and deformations in the body during a loading program which carries it from an elastic state into an elasto-plastic state and finally into a fully ideally plastic state, when deformation continues without load increase and the limiting load is thus attained. However, such an analysis is extremely difficult to perform and it is the great advantage of the theorems of limit analysis that the limiting load can be estimated by bounding from above and below without reference to the loading program by which the limiting load is attained. The limit analysis theorems have been discussed and proved in several plasticity texts. For the theorems in the plane strain case, which is of importance for the following treatment of fiber reinforced materials, see Ref. 4. For very general treatment in the three dimensional case see Ref. 5.

Fiber Reinforced Materials

Consider a fiber reinforced cylindrical specimen consisting of an ideally plastic binder and elastic-brittle fibers which are parallel to the specimen generators. The assumption of elastic-brittle fibers is certainly valid for the commonly used glass fibers.

It is assumed that the specimen is in plane strain. Under these conditions the commonly used Tresca and Mises yield conditions are the same (Ref. 4). The specimen is referred to a cartesian system of axes where the x_1 axis is in fiber direction and x_2x_3 are in the transverse plane normal to the fibers.

The yield condition for the binder material then assumes the form

$$(\sigma_{22} - \sigma_{33})^2 + 4\,\sigma_{23}^{\;2} = \sigma_y^{\;2} \qquad (10)$$

where σ_y is the yield stress of the matrix in simple tension. For convenience let the cross section of the fiber reinforced specimen be chosen rectangular and let a simple tension $\sigma_{22} = \sigma^o$ be applied to two opposite faces (Fig. 3a). The limiting load σ^L is defined as that value of σ^o for which the deformation of the specimen increases without increase in load. This load may be defined as the strength of the specimen for the loading described. The theorems of limit analysis provide a method for bounding σ^L from below and above. To find a lower bound on σ^L one has first to construct what is known as a statically admissible stress system (Ref. 1,2). It is easily realized that the stress system

$$\sigma_{22} = \sigma^o \qquad (\sigma^o \leq \sigma_y) \tag{11a}$$

$$\sigma_{33} = \sigma_{23} = 0 \tag{11b}$$

in binder and fibers is statically admissible since it satisfies the boundary conditions, equilibrium equations, traction continuity at fiber-binder interfaces and nowhere violates the yield condition (Eq. 10). Accordingly, any $\sigma^o \leq \sigma_y$ is a lower bound on σ^L and the best lower bound associated with (Eq. 11) is σ_y itself. Consequently

$$\sigma_y \leq \sigma^L \tag{12}$$

Thus the yield stress of the binder is a lower bound for the strength of the specimen under the loading described.

It follows in a completely analogous way that when the specimen surface is subjected to pure shear τ^o in the x_2x_3 plane, the strength in shear τ^L is bounded from below by $\sigma_{y/2}$, thus

$$\frac{\sigma_y}{2} \leq \tau^L \tag{13}$$

Finally if the specimen is subjected on its boundaries to biaxial stress

$$\sigma_{22} = \sigma_2^o$$

$$\sigma_{33} = \sigma_3^o \tag{14}$$

$$\sigma_{23} = 0$$

the limiting load is bounded from below according to the condition

$$\sigma_y \leq |\sigma_3^o - \sigma_2^o| \tag{15}$$

the lower bounds are geometry independent.

For upper bound construction it is necessary to construct what is known as a kinematically admissible velocity field. Consider again the specimen shown in Fig. 3a under the same loading. However, in the subsequent treatment a geometrical restriction has to be introduced. It has to be assumed that it is possible to put a plane (normal to the x_2x_3 plane) through the specimen which does not cut through any fiber. Let the inclination of this plane to the x_1x_2 plane be denoted by α (Fig. 3b).

The kinematically admissible velocity field chosen is defined by a constant velocity v of the part $\overline{aefd}$ relative to the part $\overline{efcb}$, in the direction of the cut $\overline{ef}$. Thus the velocity field is a sliding rigid body motion of one part relative to the other. There is a tangential velocity discontinuity, only, of the velocity at $\overline{ef}$ which is permitted in a kinematically admissible field.

In cartesian components the velocity field is given as follows:

$$\left.\begin{array}{l} v_2 = 0 \\ v_3 = 0 \end{array}\right\} \text{ in } \overline{efcb} \tag{16}$$

$$\left.\begin{aligned} v_2 &= -v\cos\alpha \\ v_3 &= -v\sin\alpha \end{aligned}\right\} \text{ in } \overline{aefd} \tag{17}$$

Since the velocities are constant they satisfy the incompressibility condition. Also rigid body motions are permitted for a kinematically admissible fields at those parts of the boundary where tractions are prescribed, (ref. 5). Consequently the velocity field (eq. 16,17) is kinematically admissible.

Proceeding now according to ref. 4, Chapter 7, the kinematically admissible multiplier m_k is defined by

$$m_k = \frac{\sigma_Y}{2} \quad \frac{\int_A \dot{\Gamma}\, dA + \int_{\overline{ef}} \Delta v\, ds}{\int_C (T_2 v_2 + T_3 v_3) ds} \tag{18}$$

Here A is the area abcd, $\dot{\Gamma}$ is the plastic dissipation function which depends only upon the strain rates derived from the kinematically admissible field, Δv is the tangential discontinuity in the velocity across $\overline{ef}$, ds is an element of length, C the boundary $\overline{abcd}$ and T_2 and T_3 are components of traction on the boundary. The meaning of m_k is explained by the statement that $m_k \sigma^o$ is an upper bound on σ^L. Because of the nature of eq. 16 & 17 the strain rates vanish and thus vanishes. Introducing eq. 16 & 17 into eq. 18 and using the present particular boundary loading, one finds

$$m_k = \frac{\sigma_Y}{\sigma_o} \quad \frac{1}{\sin 2\alpha} \tag{19}$$

and accordingly

$$\sigma^L \leq \frac{\sigma_Y}{\sin 2\alpha} \tag{20}$$

The maximum of sin 2 is unity, for $\alpha = 45^\circ$. In that case, combining eq. 20 with eq. 12 it follows that

$$\sigma_L = \sigma_Y \tag{21}$$

Thus, in the event that it is possible to put a 45° plane through the specimen without cutting any fibers, the strength of the fiber reinforced specimen is just the strength of the binder, independently of the shape or stiffness of the fibers.

The same situation is valid for biaxial applied stress of the type of eq. 14. In the event of applied uniform shear stress, the limiting shear stress τ^L is $\sigma_Y/2$ if it is possible to put a plane through the specimen, without cutting fibers, which is perpendicular to the direction of one of the shear stresses.

The preceding results are chiefly important for regular arrays of fibers of equal cross section. Consider for instance a square array of fibers of equal circular sections. The most unfavorable situation for uniaxial stress is at 45° to the array side (Fig. 3c), for in this case it is always possible to put a 45° plane through the binder alone. However, if the array is oriented as in Figure 3d, the possibility of putting a 45° plane through the binder alone depends on the fractional volume of fibers. It is easily found that this is possible only for a fractional volume smaller than $\frac{\pi}{8} = 0.392$.

Particle Reinforced Materials

The preceding analysis is easily carried out for the three-dimensional case of a plastic binder which is reinforced by elastic-brittle particles. In this case the theorems of limit analysis have to be used in their three dimensional form (compare ref. 5). However, in three dimensions the Tresca and Mises yield conditions are not the same, and accordingly the results are somewhat modified.

For lower bound construction the results (eq. 12, 13 and 15) are recovered identically for both yield conditions. Again the results are independent of the geometry.

For upper bound construction, the Tresca yield condition leads again to coincidence of upper and lower bounds with a geometrical restriction similar to the one used before. Thus for uniaxial stress eq. 20 is found again if it is possible to put a plane through the binder which makes an angle α with the direction of the stress. For $\alpha = 45^{\circ}$, eq. 21 is found again and analogously for biaxial stress the limiting load is defined by

$$|\sigma_i^c - \sigma_j^c| = \sigma_y \tag{22}$$

where i and j are any perpendicular directions.

For applied shear again

$$\tau^L = \sigma_y/2 \tag{23}$$

if it is possible to put a plane entirely through the binder which is normal to one of the shear stresses.

For the Mises yield condition the bounds do not coincide. Thus for simple tension with the 45° plane condition

$$\sigma_y \leq \sigma^L \leq \frac{2\sigma_y}{\sqrt{3}} = 1.15\,\sigma_y \tag{24}$$

Analogously for biaxial stress

$$\sigma_y \leq |\sigma_1^{\circ} - \sigma_1^{\circ}| \leq 1.15\,\sigma_y \tag{25}$$

and for pure shear

$$\frac{\sigma_y}{2} \leq \tau^L \leq \frac{\sigma_y}{\sqrt{3}}$$

Conclusion

It has been shown that under certain geometrical conditions, the strength of an ideally plastic binder is not increased (or increased at most by 15%) by reinforcement with elastic-brittle fibers or particles.

While the geometrical restriction that a plane can be passed through the binder without cutting the reinforcement is certainly severe, it may not be unreasonable to expect that, even if this condition is not fulfilled, the strength is not greatly increased by reinforcements localized in the form of particles or transverse fibers.

Evaluations of Directions for Improvements

An evaluation of the potential of filament reinforced composites for shells in axial compression was initiated in Ref. 6. A first tentative conclusion was that "In order to compete with shell material like 7075-T6 aluminum alloy over all loading ranges....a number of material improvements in the composites are needed." Accordingly the study has been extended to determine which areas of improvement should be most effective.

In this extension several significant refinements have been made in the methods of analysis. The detailed refinements will be described in the text to follow; the major change from the approach of Reference 6 is that effort has been concentrated upon the low end of the previously considered range of loading intensities. A review of the values of $\frac{N_x}{R}$ appropriate for boost vehicles has shown that they lie in the range 50 - 500 $\frac{KN}{m^2}$ (7.5 - 68 psi, Ref. 7). For these low loadings, the elastic buckling characteristics of the shell are of prime importance, and accordingly attention has been centered here upon the elastic buckling resistance of the composites, as will be shown.

In the following exposition, cognizance is taken of the fact that this is a progress report, not a final report, and so emphasis is placed on results and implications rather than details of execution. A complete presentation of derivations of equations and the like will be made at the end of the next quarter. With these ground rules in mind, we will describe only the development of the present assessments of composite shells, and the launch directly into the evaluation studies.

Basis for Assessment

In the elastic range, the shell weight required per unit surface area per unit radius $\frac{W/m^2}{R}$ is proportional to the square root of the loading index $\frac{N_x}{R}$, thus

$$\frac{W/m^2}{R} = F\sqrt{\frac{N_x}{R}} \tag{26}$$

For filamentary composite sandwich shells the value of F may be derived from the results of Stein and Mayers (Ref. 8)

$$F = \frac{\rho_s + \rho_c\left(\frac{t_c}{2t_s}\right)_{opt}}{\sqrt[4]{\left[\left(\frac{t_c}{2t_s}\right)_{opt}+1\right]^3 - \left(\frac{t_c}{2t_s}\right)^3_{opt}}} \left\{\frac{E_L E_T}{3(1-\nu_{LT}\nu_{TL})}\left[\frac{1+\sqrt{\frac{E_L}{E_T}}\left\{\nu_{LT}+2(1-\nu_{LT}\nu_{TL})\frac{G_{LT}}{E_L}\right\}}{1+\frac{1}{2}\sqrt{\frac{E_L}{E_T}}\left\{\frac{E_L}{G_{LT}}-2\nu_{TL}\right\}}\right]\right\}^{-1/4} \tag{27}$$

where $\left(\frac{t_c}{2T_s}\right)_{Opt}$, the optimum proportions of core thickness to face thickness, may be found from the expression

$$\frac{\rho_c}{\rho_s} = \frac{2\left(\frac{t_c}{2t_s}\right)_{opt}+1}{2\left(\frac{t_c}{2t_s}\right)^2_{opt}+3\left(\frac{t_c}{2t_s}\right)_{opt}+\frac{4}{3}} \tag{28}$$

Equation (26) indicates that the efficiency of various shell structures for resisting elastic buckling may be compared by comparing the value of F pertinent thereto - the lower the value of F, the more efficient the structure.

Because optimal directions for property improvement are not obvious from inspection of equation (27) for F, a comprehensive study of the effects of varying the properties of the constituents of filament reinforced composite has been programmed for the IBM 1620 and 7090 computers. This program utilizes the results of the analysis of elastic constants obtained in Ref. 1 together with equations (27) and (28), and the first results will be reported in the following section of this report.

As a basis for comparison, the efficiency of cylinders with metal-faced sandwiches were also calculated. For the isotropic metal faces, the expression for F, comparable to equation (27) is simply:

$$F = \frac{\rho_s + \rho_c\left(\frac{t_c}{2t_s}\right)_{opt}}{\sqrt[4]{\left[\left(\frac{t_c}{2t_s}\right)_{opt}+1\right]^3-\left(\frac{t_c}{2t_s}\right)^3_{opt}}} \quad \frac{1}{\left[\frac{E}{\sqrt{3(1-\nu^2)}}\right]^{1/2}} \tag{4}$$

In order to provide as firm a foundation as feasible for comparison, an effort was made to cover the range of structural metals potentially applicable to boost-vehicle construction. Possibly optimistic properties were assigned to the metals chosen in an effort to compensate for near future improvements, and the family of materials having the properties given in Table 1 was selected as characteristic of current and near future aerospace metals. These properties were employed in the cylinder efficiency equations described, with the additional assumptions of (1) buckling at the yield stress if the elastic range was exceeded and (2) of the use of an ideal sandwich core material with density 277 $\frac{kg}{m^3}$ (.001 psi) to yield the curves plotted as Figure 4.

From Figure 4 the following results, which will be used in the subsequent sections as the basis for the assessment of composites, are derived.

1. The good structural metals (the steel, titanium and beryllium alloys used) all make comparably efficient sandwiches at loading intensities appropriate for large boost vehicles (as for the SaturnV shown in Fig. 4). This efficiency corresponds to an F value for an elastic material of 0.025 $\frac{N^{1/2}}{m^2}$ (0.0011 $\frac{pef/in}{psi^{1/2}}$), and this value of F will be used as a reference (F_{Ref_1}) hereinafter to measure the efficiency of composites. Thus, composites having F values greater than F_{Ref_1} are not competitive with metals for this application, and only those directions for improvement pointing toward lower F-values are deserving of greatest emphasis.

2. Even at the low loadings of boost vehicles, optimally proportioned metal-faced sandwich cylinders are in general stressed to the yield stress. At the lowest value of $\frac{Nx}{R}$ known to be of practical interest (that for the Atlas vehicle as shown on Fig. 4), the equivalent elastic F values for the materials considered are as follows:

Material	F, $\frac{N^{1/2}}{m^2}$	$\frac{pef/in}{psi^{1/2}}$
Be	0.012	(0.00053)
Steel	.020	(.00088)
Al	.020	(.00086)
Ti	.022	(.00097)
Mg-Li	.027	(.0012)

Thus while composite materials which can achieve F-values less than 0.025 $\frac{N^{1/2}}{m^2}$ are of interest for the more heavily loaded boost vehicles like the Saturn V, they need to achieve somewhat lower values for more lightly loaded cases like the Atlas.

In the following sections the composites will generally be related to the F_{Ref_1} value of 0.025 $\frac{N^{1/2}}{m^2}$. The need for somewhat lower values to be competitive in the lowest loading intensity regimes should not be forgotten, however. Particularly the especial effectiveness of beryllium for these cases should be borne in mind. The reservation should also be remembered that the restriction (limited to this reporting period) to a hypothetical case of density 277 $\frac{kg}{m^3}$ for the sandwiches may have some - but perhaps not profound - influence on the

Constituent Properties Considered

The variables considered in this assessment of materials for the constituents of composites included filament moduli and densities, binder moduli, volume fraction of binder, and two filament orientations. Filament properties were chosen as idealized representations of "available" materials. Binders derived from the properties of epoxy resins with hypothetical fiber materials to investigate parametrically the effect of a change in binder modulus with no change in binder density. Properties used for filaments and binders are given in Table 2. Volume fraction binder was varied from zero to one hundred percent, but only two filament orientation configurations were considered in the light of previous results (Ref. 4) which suggested that orientations other than "0^o" (all filaments in the loaded direction) and "isotropic" (three layers with filament 0^o and $\pm$ 120^o to the load) were of lesser interest.

Values of F were calculated for all combinations of the above variables using the equations and methods discussed in the preceeding section. The results are plotted in Figure 5-8.

Results and Discussion

Figures 5-8 present the results as plots of values of F versus volume ratio of binder to composite. On all figures a horizontal line is drawn at the value of F_{Ref_1}; thus below the line the properties are of interest of boost-vehicle applications from a structural efficiency standpoint.

The effect of the various changes in constituent properties on the resulting values of F have a number of implications for future directions of research. These results will be considered first as regards their general implications and second in more detail, separately variable by variable.

General Implications

1. Advanced composites are needed to be competitive with present highly developed metal for compressive cylindrical shell applications requiring lightly loaded sandwich construction. If one accepts the high-modulus glass in 30% by volume epoxy resin as representative of the present advancement of composites, one finds that it just barely surpasses the value of $F_{Ref\,1}$ in the isotropic configuration.

2, Directions for improvement are not readily determined in advance from simple constituent characteristics such as modulus to density ratio but require a detailed survey of the present kind. For example, the modulus to density ratio for steel is not substantially different from that for E-glass, but the F-values for steel reinforcement vary from less than those for E-glass (high-binder content, low modulus binder isotropic configuration) to much more than those for E-glass (low binder content, low modulus binder, 0^o configuration) and even run higher in some cases than those for the binder alone for the high modulus binders.

3. A wide variety of combinations of the properties considered can yield composites having F-values less than $F_{Ref\ 1}$ particularly with the isotropic configuration. Thus potentially composites should be most suitable for boost vehicle applications. (The exception to this implication is provided by beryllium for the most lightly loaded vehicles; here only the most advanced composites have the potential of being competitive.

Perhaps of more immediate significance than such general implications as the foregoing are the specific implications arising from the relative position of the curves denoting the relative merits of various possible improvements. These will be discussed in the following section.

<u>Specific Implications</u> - 1. <u>The isotropic configuration</u>

The isotropic configuration is remarkably more effective than the 0^o configuration for this buckling application, - especially for the lower (and presently more realistic) modulus binders. While studies need to be concluded to verify the preliminary results of Reference 4 that some other configuration is not competitive, the present results suggest that for the buckling of cylindrical shells emphasis should be upon the isotropic laminates. Studies of the possible influence of intra-laminar shear effects upon this conclusion are also required.

2. <u>Binder content</u> - With the isotropic configuration, the achievement of high packing densities is less vital to the achievement of low F-values than for the 0^o configuration. Indeed the use of relatively small volume percentages of high-modulus filaments like boron or alumina to a low-modulus binder can produce F-values well below the $F_{Ref\ 1}$ when the isotropic configuration is used. If glass filaments are used, however, high packing

densities are required. Perhaps the most astonishing variations with binder content are those exhibited by the (high density) steel reinforcements. Although the losses in efficiency shown by the rising F-values with decreased binder content at high binder moduli are not unexpected (see Fig. 5) the reversals in the curves at high binder content for the lower modulus binder was a surprise to the authors, as was the fact that with the isotropic configuration steel excelled E-glass in some ranges (Fig. 6). For all materials, in any case, the lowest values of F were associated with the highest filament concentration (lowest binder content), but small concentrations of alumina or boron may be better than high concentrations of glass (see Fig. 3).

3. Filament Properties - As expected for this application steel filaments generally gave the highest F-values and boron filaments the lowest. While E-glass requires packing ratios which are probably impractically high to give F-values below $F_{Ref\ 1}$ unless a better binder than epoxy is available, normal proportions of glass with a Young's modulus of 11 $\frac{GN}{m^2}$ (16,000,000 pse) as well as boron and alumina in low concentration (in the isotropic configuration) should be capable of performance at least equivalent to metals for large booster applications. Substantially better performance than metals should be accessible with high-modulus glass filaments with improved binders. (Improved binders are not needed with boron or alumina filaments. See next section).

4. Binder properties - Improvements in binder modulus are less effective in reducing F-values of isotropic laminates than was anticipated at the initiation of this study. Doubling the Young's modulus, from 3.45 $\frac{GN}{m^2}$ to 6.9 $\frac{GN}{m^2}$ (1/2 to one million psi) does bring E-glass into contention as a

possible reinforcement for advanced sandwich shell (see Fig. 6); it makes the achievement of a possible 20% weight saving from metals for large booster conceivable with high-modulus glass in high concentration. If advanced filaments like boron or alumina are employed however, improving the binder makes very little change in the F-value for the composite (see Fig. 6) If non-isotropic laminates are required the binder modulus effect increases in importance.

5. Hollow fibers - The special case of hollow fiber (inside radius = 80% outside radius) is considered in Figures 7 and 8. For this lightly loaded sandwich shell application hollow fibers are contra-indicated; with the isotropic configuration they lead universally to heavier structures. (This result may be reversed if heavier core densities are used for the sandwiches)

CONCLUSIONS

The rational evaluation of elastic constants for arbitrary phase geometries will require a statistical definition of geometry to yield useful numerical results. The previously obtained random array results are somewhat modified by the present arbitrary transverse geometry bounds and, as modified, they represent the most practical expressions available for evaluating plastic moduli.

Significant practical variations in matrix properties through the use of particulate additives appear to be attainable although the effect on strength is not yet well understood.

The present status of the structural efficiency studies enables one to draw the following conclusions:

1. Advanced filament reinforced composites have the potential to exceed the structural metals in efficiency as cylindrical shells for carrying the compressive loadings of typical launch vehicles.

However,

2. To be competitive with metals, composites must have improved properties compared to present E-glass reinforced epoxies. The improvements do not have to be extreme, however. For example, the use of high-modulus glass filaments either with better packing ratios than present

practice or in a binder of higher modules than epoxy can yield a booster-shell material potentially more efficient than metals.

3. An "isotropic" reinforcing configuration is generally more effective in a shell for resisting elastic buckling than a shell with longitudinal and circumferential filaments. The improvement associated with the isotropic configuration varies with reinforcement properties and binder content. Most substantial is this improvement when the ratio of filament modulus to binder modulus is large and the binder content is also large.

In consequence of 3:

4. The use of high-modulus fila[illegible]ts (boron, alumina) in an isotropic configuration in a resin like [illegible] will produce elastic buckling efficiencies of cylindrical shell structures superior to metals with very low percentages of reinforcement.

5. Steel filaments do not appear suited to use for the reinforcement of cylindrical shells in compression. The same conclusion applies to hollow glass filaments when used in the facing of sandwiches having low density cores.

References

1. B. W. Rosen, N. F. Dow and Z. Hashin -- "Mechanical Properties of Fibrous Composites". Contract NASW 470, NASA Report CR-31, April (1964).

2. Z. Hashin and B. W. Rosen -- "The Elastic Moduli of Fiber-Reinforced Materials". Journal of Applied Mechanics, Vol. 31E, pp. 223-232, June (1964).

3. Z. Hashin and S. Shtrikman -- "On Some Variational Principles in Non Homogeneous and Anisotropic Elasticity". Journal of Mech. Phys. Solids, Vol. 10, pp. 335-342, (1962)

4. W. Prager and P. G. Hodge -- "Theory of Perfectly Plastic Solids". J. Wiley and Sons, (1951)

5. W. T. Koiter -- General Theorems for Elastic-Plastic Solids -- Chapter IV in "Progress in Solid Mechanics." Sneddon and Hill, Eds. North Holland, (1960).

6. Dow, Norris F., and Rosen, B. Walter. "Study of the Relationship of Properties of Composite Materials to Properties of Their Constituents." Quarterly Program Report No. 1, Jan. 24, 1964, on Contract NASW-817

7. Anderson, Roger A. Private Communication. Feb. 5, 1964

8. Stein, M.; and Mayers, J. "Compressive Buckling of Simply Supported Curved Plates and Cylinders of Sandwich Construction." NACA TN2601, Jan. 1952.

TABLE 1

FORMULATIONS AND MECHANICAL PROPERTIES

Series	Resin Component		Filler	UTS	Elongation	Mod. psi
19	Kopoxile 159 MNA EM207 BDMA	100 pbw 125 pbw 75 pbw 1 pbw	Unfilled	5.68-5.90	10	$2.77\text{-}2.84\times10^{5}$
18	Same		66% (weight) Al powder as received	4.80-5.24	0.87-1.12	$0.88\text{-}1.26\times10^{6}$
22	Same		Same washed in acetone and ligroine	5.10-5.64	0.67-0.83	$1.08\text{-}1.32\times10^{6}$
23	Same		Same coated with mold release	3.52-4.57	0.35-0.66	$0.89\text{-}1.31\times10^{6}$
24	Kopoxite 159 MNA EM207 BDMA A1100	100 pbw 125 pbw 75 pbw 0.5 pbw 1.5 pbw	66% aluminum powder, decreased by washing in ligroine and acetone	2.35-2.74	5.3-9.7	$3.75\text{-}5.6\times10^{5}$
28	Same as Series 24		Same as Series 24	4.88-5.05		
29	Substitution of 26020 for A1100 in Series 24		Same as Series 24	Not tested - Casting contained voids		
30	Kopoxite 159 MNA EM207 BDMA	100 pbw 125 pbw 75 pbw 1 pbw	66% aluminum powder, conversion coated by Detrex wash and chromate etch	6.15-6.40		

TABLE 1 (continued)

Series	Resin Component		Filler	UTS	% Elongation	Mod. psi
31	Repeat of Series 29		Repeat of Series 29	3.84-3.88		
12A-28-1	Same as Series 19 and 30		None	5.95	11	3.08×10^5
12A-28-2	Repeat of Series 30		Repeat of Series 30	6.05-6.60	1.1-1.5	$7.61-10.5 \times 10^5$
12A-29-5	Kopoxite 159	100 pbw	Same as Series 30	5.47-6.12	0.5-0.62	$1.61-2.28 \times 10^6$
	MNA	125 pbw				
	EM207	25 pbw				
	BDMA	1 pbw				
12A-29-6	Same as 12A-29-5		None	9.98-12.1	2.52-5.4	$4.38-5.09 \times 10^5$

Table 2 - Properties of idealized metals used as basis for assessment of composites

Metal	Young's Modulus, E $\frac{GN}{m^2}$	(ksi)	Compressive Yield Stress, cy $\frac{MN}{m^2}$	(psi)	Density, C $\frac{Mg}{m^3}$	(pci)	Poisson's Rat.
Magnesium - Lithium Alloy	42.75	(6200)	124.1	(18,000)	1.342	(0.0485)	0.43
Beryllium	293	(42,500)	400	(58,000)	1.827	(.066)	.09
Aluminium Alloy	73.78	(10,700)	482.7	(70,000)	2.796	(.101)	.315
Titanium Alloy	103.4	(15,000)	1379	(200,000)	4.816	(.174)	.145
Steel	206.9	(30,000)	2069	(300,000)	7.833	(.283)	.25

Table 2 - Properties of idealized filaments and binders used for composites

Filament	Young's Modulus, E $\frac{GN}{m^2}$	(ksi)	Compressive "Yield Stress", cy* $\frac{MN}{m^2}$	(psi)	Density, C $\frac{Mg}{m^3}$	(pci)	Poisson's Rati
Steel	206.9	(30,000)		( )	7.833	(0.283)	0.25
E-Glass	72.40	(10,500)	1034	(150,000)	2.530	(0.0914)	0.20
Hi-Mod. Glass	110.3	(16,000)	1276	(185,000)	2.530	(0.0914)	0.20
Boron	344.8	(50,000)			2.297	(0.083)	
Alumina	517.1	(75,000)			3.958	(0.143)	
Binder							
I	3.45	(500)	----		1.273	(0.046)	0.35
II	6.9	(1,000)	----		1.273	(0.046)	0.35
III	13.8	(2,000)	----		1.273	(0.046)	0.35
IV	27.6	(4,000)	----		1.273	(0.046)	0.35

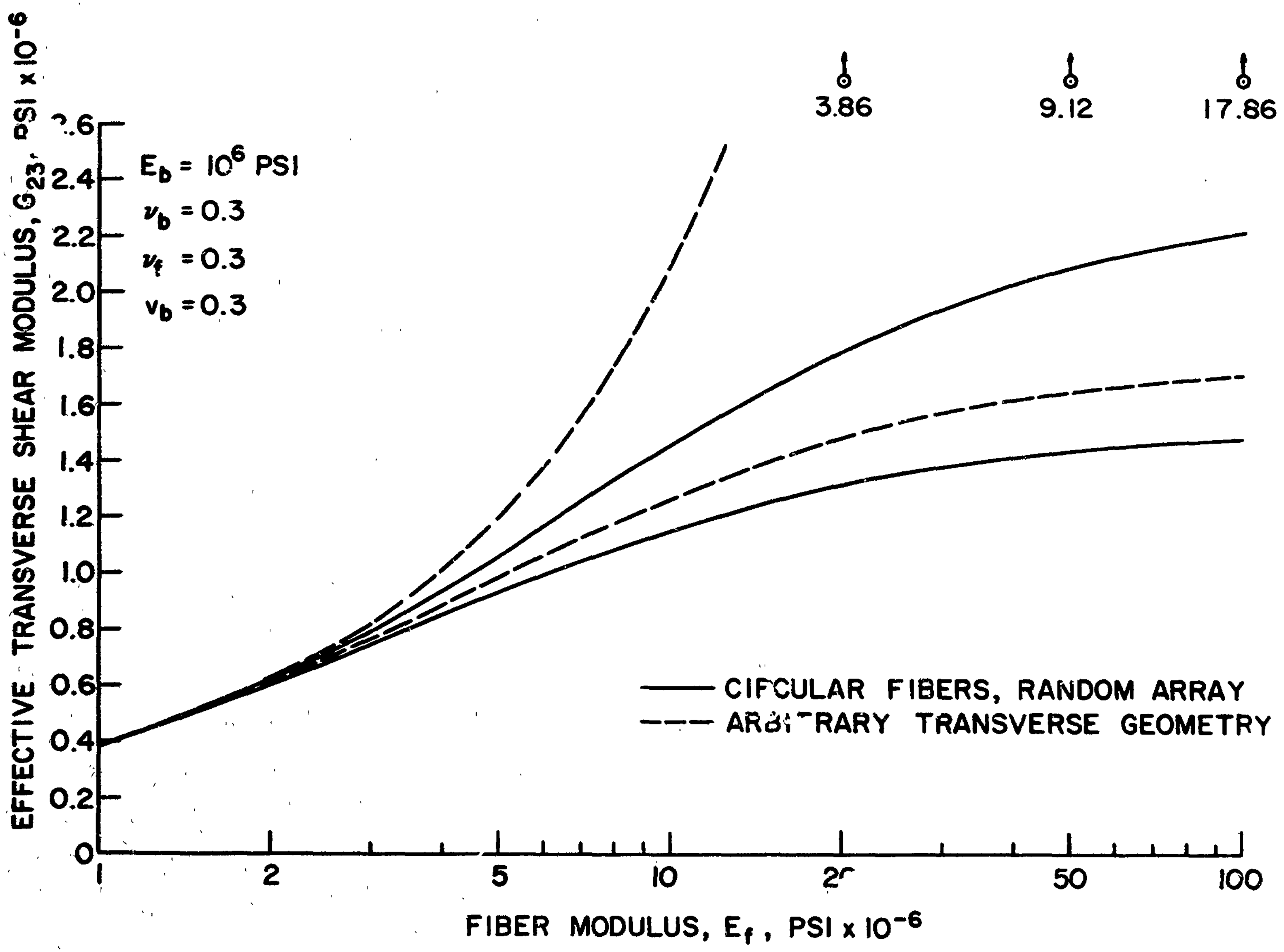

Figure 1. Comparison of Effective Transverse Shear Modulus Bounds Based on Arbitrary Transverse Geometry with the Bounds for a Random Array (Ref. 1 & 2).

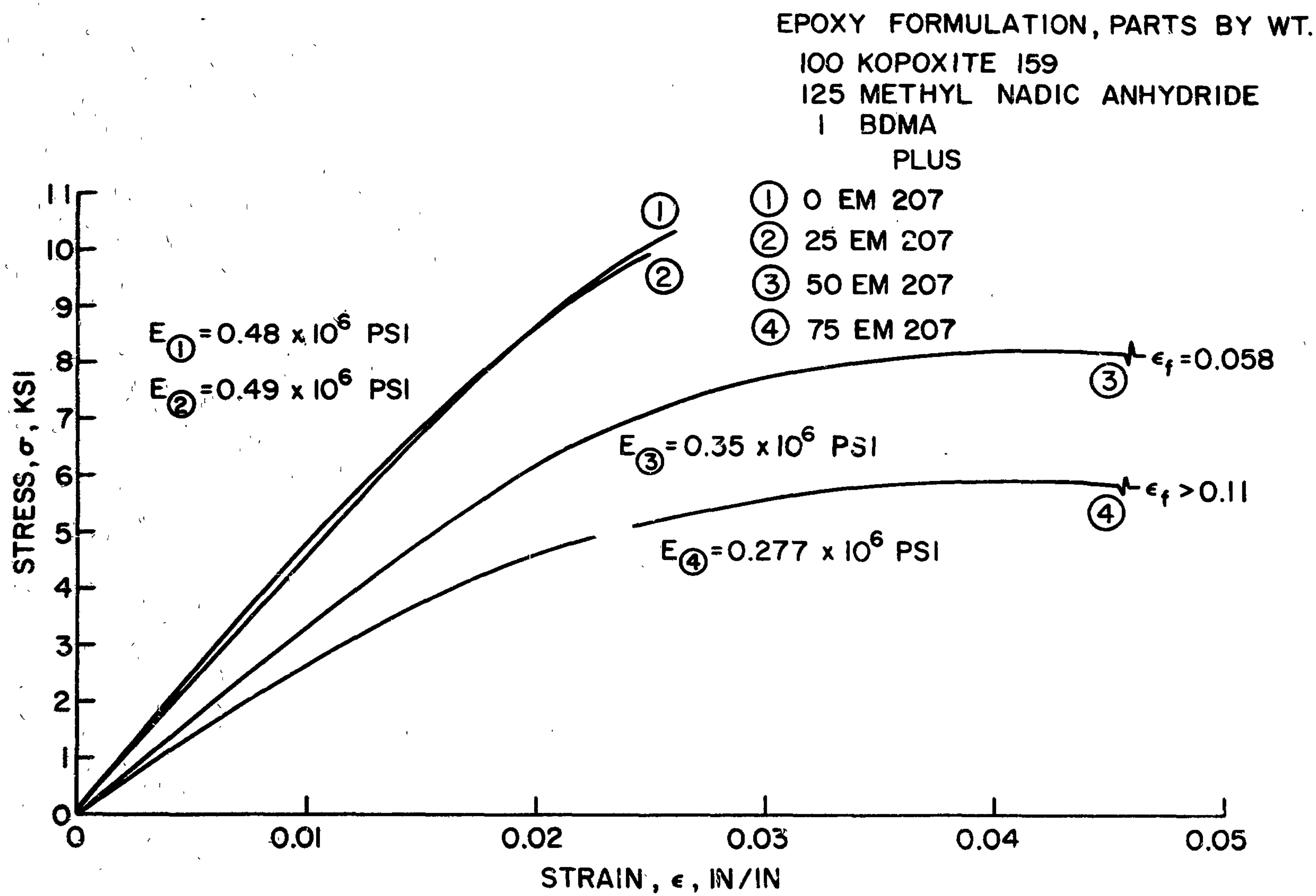

Figure 2. Stress-Strain Curves for a Series of Epoxy Materials.

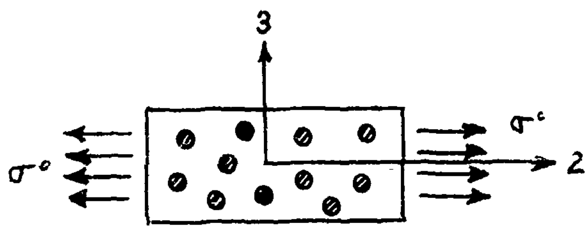

Figure 3a.

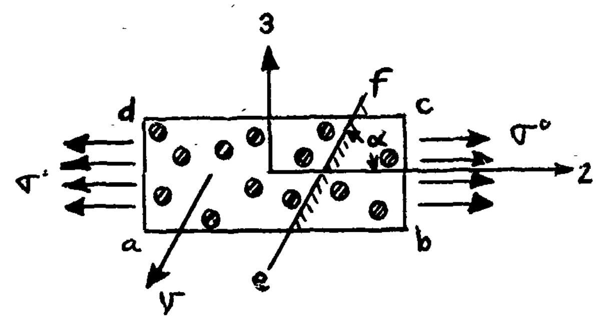

Figure 3b.

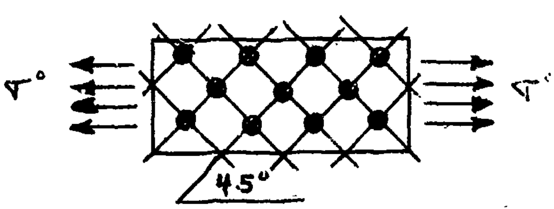

Figure 3c.

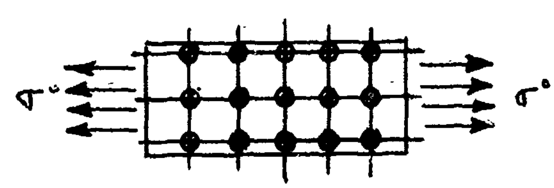

Figure 3d.

Figure 3. Geometries Considered for Limit Analysis.

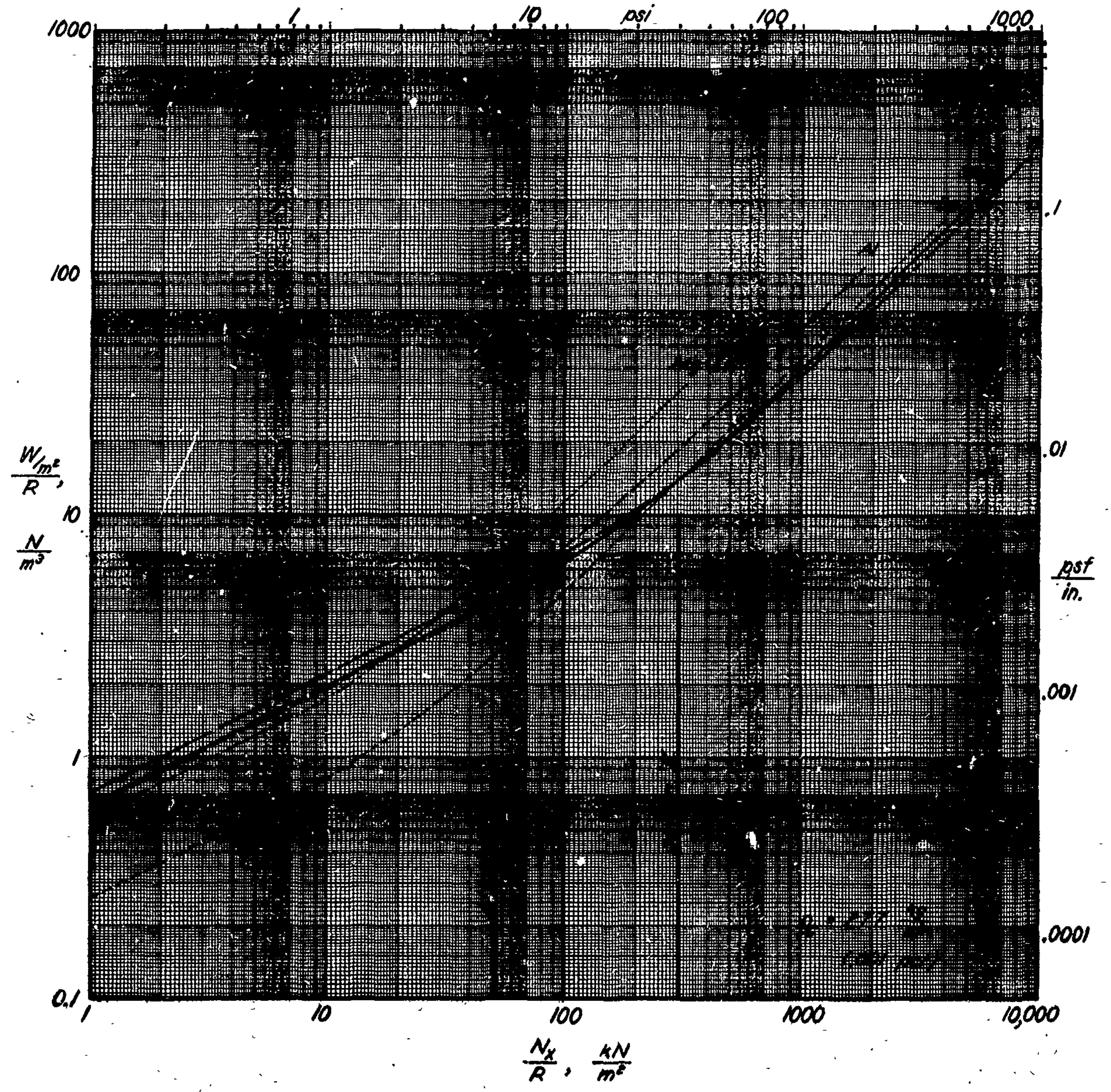

Figure 4. Efficiencies of Structural Metals for Sandwich Construction of Cylindrical Shells in Compression.